Materials Research Proceedings 41 (2024) 1123-1134 https://doi.org/10.21741/9781644903131-124

Residual formability analysis of bent and remanufactured thin steel sheets

FARIOLI Daniele[1,a*], KAYA Ertuğrul[1,b], STRANO Matteo[1,c]

[1]Politecnico di Milano, Department of Mechanical Engineering, Via La Masa 1, 20156 Milano

[a]daniele.farioli@polimi.it, [b]ertugrul.kaya@polimi.it, [c]matteo.strano@polimi.it

Keywords: Residual Formability, Automotive Steel, Remanufacturing, V-Bending, Flattening

Abstract. This study examines the plastic deformation and remaining formability of DC04 mild steel, a material frequently used in automotive applications, after undergoing V-bending and subsequent cold or warm flattening processes. The research aims to determine if previously bent sheets maintain sufficient ductility for an additional forming cycle, a key factor in advancing circular economy practices. Samples were cold-formed into V-bends of various angles and then reshaped through flattening, with critical process parameters controlled. Tensile tests were performed on both the original sheets and reshaped samples to study the impact of the bending index, dwell force, dwell time, and flattening temperature on mechanical properties. Geometric characterization of the samples before and after flattening showed localized permanent deformation and an "M" profile near the bend line, leading to a spring-forward effect and a "U" shape of the samples. Analysis of tensile stress-strain curves and regression models indicated a decrease in elongation at maximum stress with an increasing bending index, while the ultimate tensile strength remained relatively constant. Yield stress showed a minor increase with a higher bending index and flattening temperature. These results underscore the potential for reusing end-of-life vehicle sheets, providing a more sustainable alternative to conventional recycling methods.

Introduction.

Formability is the ability of a given metal workpiece to undergo plastic deformation without failure [1]. According to Small et al., formability can be defined as a probability of failure, proposing the concept of "forming maps", which showed how failure risk increases with major strain [2]. Automotive industries are interested in the formability of sheets, especially in the context of multistage stamping [3]. Ensuring successful forming, sufficient post-process residual ductility, and enhancing the strength of lightweight car bodies brought the development of special alloys such as aluminum alloys and third-generation advanced high-strength steels [4]. Beyond the total tensile elongation, factors such as presswork hardening, anisotropy ratio, strain rate sensitivity, uniform elongation, edge sensitivity, and internal stress between phases play critical roles in determining the formability of complicated stress and strain distributions [4]. One practical issue is that high-strength sheet materials are often sensible to edge cracks. Because of this, many edge crack testing methods were developed [5]. Despite many new concepts of formability prediction, strain-based Forming Limit Diagrams (FLD) are used most often in engineering practice to assess sheet formability. FLDs can be determined by different methods, including experimental, theoretical, as well as hybrid methods [6]. Theoretical methods are based on criteria of the loss of stability (strain localization) or damage (fracture) of the material. In general, the most appreciated and reliable methods used are Erichsen, Marciniak, and Nakazima tests [6].

Such tests are based on Digital Image Correlation (DIC) performed with automatic strain measurement systems (AutoGrid, ASAME, or ARAMIS) and inverse parameter identification [6]. Other methods are based on stress measurement using X-ray diffraction during the Marciniak punch test [7]. The strain path dependency, a drawback of FLCs, led to the proposal of the

Generalized Forming Limit concept (GFLC), allowing for easy evaluation of formability in multi-step deformation histories. Stoughton and Yoon proposed a new failure prediction criterion by combining σFLC and the maximum shear stress (MSS) criterion, introducing the "polar diagram of the effective plastic strain" (PEPS) concept, which is path-independent and successfully implemented in commercial Finite Element (FE) codes [7].

Moreover, for most sheet materials under these complex loading processes, a strong Bauschinger effect is observed, where the material hardening behavior tends to be anisotropic [8]. The phenomenon stands in the formation and interaction of dislocation structures on the micro-structural level which can be in turn modeled by evolving structural tensors [9]. Anisotropic hardening demonstrated to predict better the spring-back of parts with respect to isotropic hardening [7]. The experimental validation for anisotropic hardening consists of multiaxial experiments, shear test and plane strain tension test, hydraulic bulge test, biaxial stress test using cruciform or tubular specimen, combined use of simple mechanical tests, in-plane compression and reverse loading tests and hole expansion forming [7].

Motivation of the research.

Most of the scientific literature presented focuses on the formability of sheets starting from the "as-received" state. At the same time, cold recycling and remanufacturing of sheet metals is an emerging area mainly because of environmental concerns: despite the proven benefits of recycling, sheet metal remelting is still a practice affected by relevant CO_2 emissions. If these "wastes" are recycled, reused, remanufactured, or repurposed by a cold process, i.e., a non-melting process, the amount of CO_2 emission can be reduced significantly [10], [11]. Employing cold recycling also allows for substantial energy savings compared to manufacturing from new materials [12]. Because of this, reusing and reshaping end-of-life sheets or pre-formed sheets by cold metal recycling routines gained significant interest over the past 15 years, with gradual progress being made by several Scientists. Furthermore, it has been demonstrated that regions of minimally deformed panels still retain significant residual life, enabling the extraction of sheets with retained ductility for subsequent remanufacturing processes under a Circular Economy perspective [11].

To deal with the issue of quantifying the formability of remanufactured sheets, Falsafi et al. proposed a reformability index. This index represents possible levels of strains for deformation along different paths, based on Polar Effective Plastic Strain (PEPS) [13]. Takano et al. studied the feasibility of cold recycling of sheet-metal wastes, finding that a forming limit of flattened sheet metals is similar to that of a sheet metal with uniform thickness [14]. Tekkaya et al. analyzed the remanufacturing of a contoured sheet metal part using a hydro-forming technology concluding that this technique applies to a re-use of sheet metal formed parts such as car bonnets [15]. Farioli et al. [11] demonstrated how to reshape successfully curved thin steel sheets into flat parts by cold and warm flattening. The process described in the paper is meant to exploit the residual material formability of automotive sheets under a circular economy perspective.

Following an approach similar to [11], this study investigates the plastic deformation and residual formability of DC04 mild steel, a prevalent material in automotive applications, subjected to V-bending followed by either cold or warm flattening processes. Examining the impact of V-bending on rectangular specimens is meant to replicate at a "small scale" specific geometrical feature typical of automotive sheet metals. Understanding the residual life and formability of these materials is crucial for circular economy applications, where materials are employed for a second life cycle and where sheet metal formability can be affected by the temperature of the dies and geometrical conditions [16]. Therefore, this article aims to test experimentally the residual formability of previously bent sheets, i.e. to assess whether they retain adequate ductility for another forming cycle.

Experimental procedure and materials.

Experiments were conducted to understand the potential of reshaping and giving sheet metal components a second life by remanufacturing. Specifically, samples of tensile test shapes (Figure 2) were extracted from 0.8 mm thick cold-rolled DC04 steel using waterjet cutting.

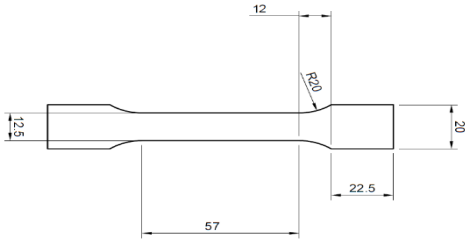

Figure 2. Geometry of the tensile test samples (mm).

Figure 1. V-bending of the tensile test samples.

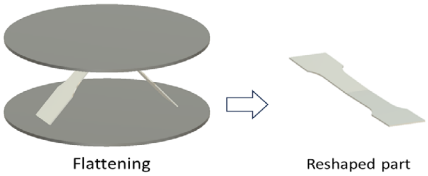

Figure 3. Flattening bent samples for obtaining a reshaped part.

These samples were cold-formed to produce V-bends of varying angles by varying the punch stroke (Figure 1). The punch performs an air-bending operation without bottoming at a controlled and constant rate equal to 3 mm/min. two stroke values, or "Bending Indexes" BI (mm) were tested in these experiments. The flattening process was then employed as a manufacturing method to reshape these parts for potential reuse. The flattening process is characterized by three main parameters. The first parameter is the dwell force DwF (kN): it is the maximum constant flattening force applied. While the upper flattening tool goes down at a constant and controlled rate (50 mm/min), the V-bent sample initially unbends and when it starts getting flat the force increases steeply. When the force reaches a predefined value, namely the dwell force, such load is kept constant for a set time, called dwell time. The second parameter is the dwell time τ (s): it is the time for which the dwell force is applied. The third parameter is the temperature T (°C): it is the temperature of the tools and of the chamber where flattening occurs. Such value is kept constant and controlled. Both V-bending and flattening have been conducted onto the MTS servo-hydraulic monoaxial testing machine: flat hard tool steel dies have been used for flattening and specific punch and matrix for V-bending operation (Figure 5). Flattening tests have been performed both in cold (20°C) and warm (250°C) conditions, by using a closed chamber with controlled and fixed temperature (Figure 4).

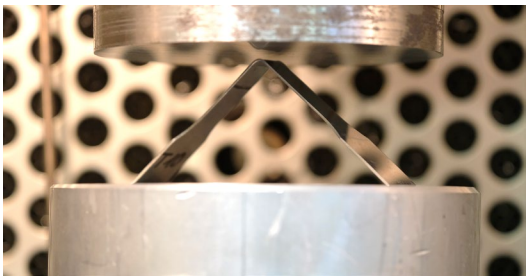

Figure 4. The picture at the beginning of flattening one sample in a controlled-temperature chamber.

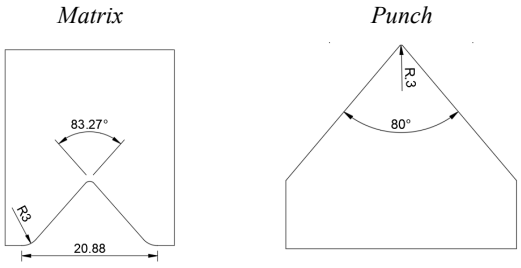

Figure 5. 2D drawing of the V-bending tools (mm).

Tensile tests have been performed onto MTS machine Alliance RT/100 as described in Figure 6 and Figure 7. The elongation rate applied is $\dot{\Delta}l = 5\ mm/min$.

Figure 6. Experimental setup for tensile tests.

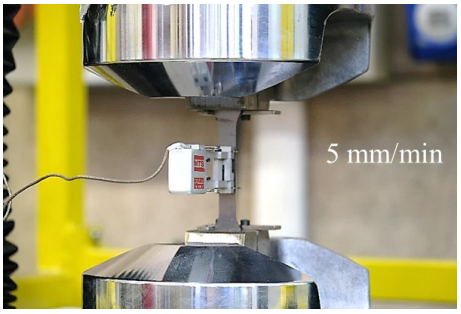

Figure 7. Zoomed view of the sample with an extensometer.

Such tests have been performed both on the as-received sheets and the V-bent and flattened samples. This procedure allows for characterizing the work-hardening and the residual tensile formability of re-shaped parts when compared to the as-received material.

Design of experiments.

This paragraph is meant to explain the parameters used during the experimental procedure (V-bending + flattening) and the sequential stages of deformations experienced by the samples (Figure 8). The factors varied during the experiments: the Bending Index (BI), the Dwell Force (DwF), the Dwell time (τ) and the Flattening Temperature (T). For each factor, two levels have been tested. For each combination of levels and factors, one replica was tested for the V-bent and flattened samples. Right after the flattening process, the samples were tested in tension to get the stress-strain curve. The as-received material has been tested in tension without performing any preliminary deformation and re-shaping. In total, 19 samples have been tested according to Figure 9: 16 samples for characterizing the effect of bending + flattening on the work hardening of the material and 3 samples for characterizing the as-received one. The response variables of interest for the tensile tests were the Ultimate Tensile Strength (UTS, [MPa]), the yielding stress (Ys, [MPa]), the Young's modulus (E, [GPa]) and the elongation at maximum stress (A%, [-]). Such response variables, together with the $\sigma - \epsilon$ diagram, can be extracted directly by the Software which controls the tensile test machine, without the need for any post-processing operation on the experimental data.

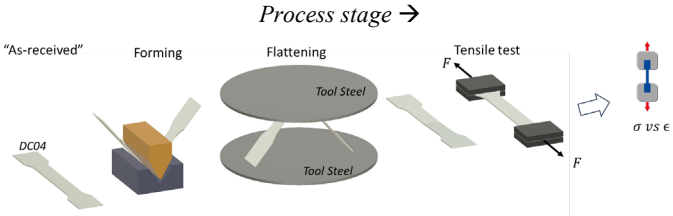

Figure 8. Deformation stages experienced by the material tested.

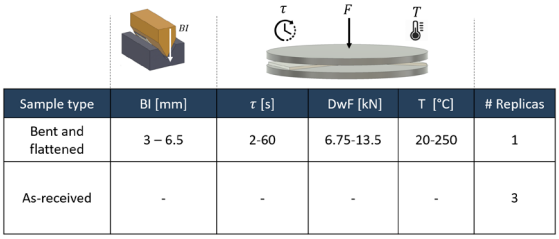

Sample type	BI [mm]	τ [s]	DwF [kN]	T [°C]	# Replicas
Bent and flattened	3 – 6.5	2-60	6.75-13.5	20-250	1
As-received	-	-	-	-	3

Figure 9. Design of Experiments followed.

Geometrical characterization of the samples.

The V-bending operation induces in the material different levels of plastic deformation according to the stroke applied by the punch. Consequently, in correspondence with the bent zones, different curvatures for the samples are obtained, therefore plastic strain distributions are obtained. To

measure such curvatures and to understand the way the specimen deforms during the forming and re-forming cycle, the samples have been characterized with Alicona Infinite Focus, as described in Figure 10. Alicona is a commercial tool that can be used for surface topography measurement. The output of the measurement is an .STL file, which can be directly analyzed by the Software developed by Alicona Brucker (Figure 11). In this specific case, the measurements were performed in two moments. Firstly, after bending, to understand the curvature and angle of the specimen. This is an indirect measure of the damage experienced by the material because of plastic deformation. The second measurement were performed after flattening, to understand the mechanics of deformation of the specimens.

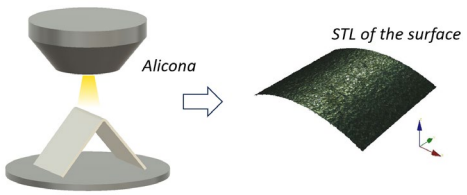

Figure 10. Positioning the sample for the geometrical analysis.

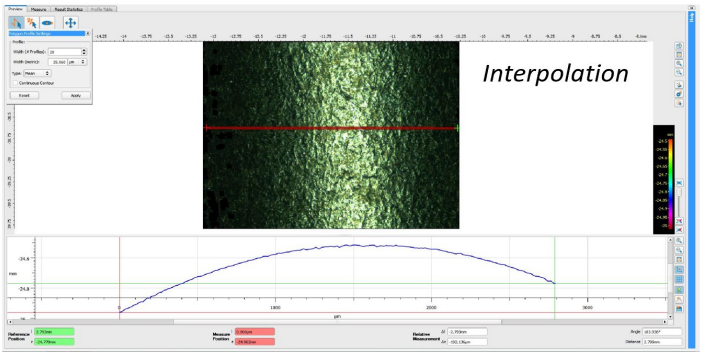

Figure 11. Interpolation of the external curvature of the sample (in .STL format) directly through the Alicona Brucker Software.

As mentioned previously, after scanning all the bent samples, two geometrical features have been measured: the external curvature radius (Figure 12) and the angle of the bent samples (Figure 13).

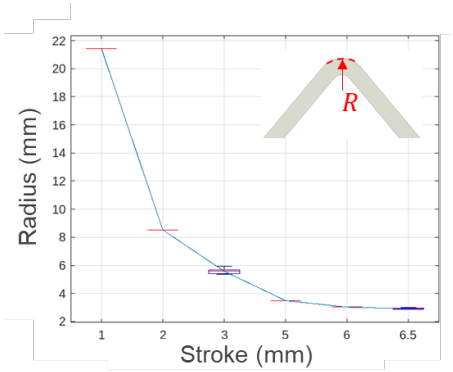

Figure 12. The geometrical relationship between external curvature radius and bending stroke.

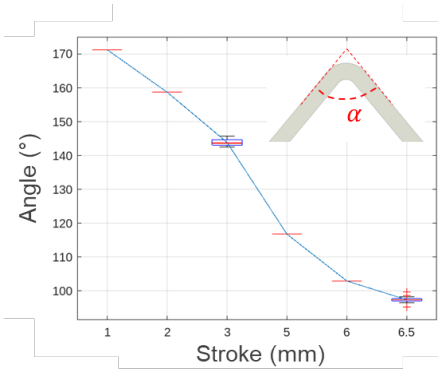

Figure 13. The geometrical relationship between bending angle and bending stroke.

Clearly, Figure 12 shows how the external curvature radius of the sample decreases (i.e. the bent line gets sharper) by increasing the stroke in the bending phase. This also denotes an increased level of plastic deformation in the material. Similarly, Figure 13 reveals that the angle of the samples after spring-back reduces by increasing the bending stroke. The trends in the two figures are analogous, implying that a correlation between angle and curvature radius exists. Lastly, Alicona has been used to analyze the bent (and unbent) line post-flattening with two aims: firstly, to deduce the deformation history of the sample during flattening and understanding how flattening modifies the shape of the sample by applying a mix of un-bending and localized compression (Figure 15). Secondly, Alicona was used to quantify the spring-back of the samples. The samples

have been positioned (through specific supports) in a way that the sample could be observed laterally, i.e. along the plane of the thickness of the blank (Figure 14).

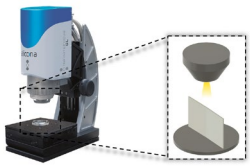

Figure 14. Positioning the sample for the geometrical analysis with Alicona.

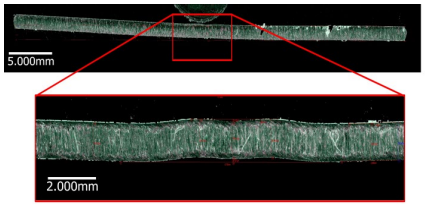

Figure 15. Sample scanned with Alicona with a zoom close to the flattened central area.

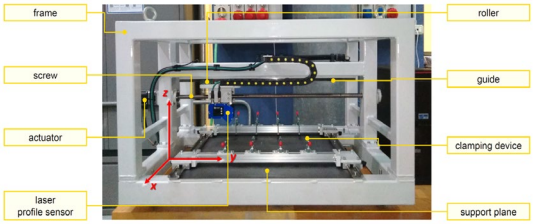

Figure 16. Laser-based profilometer used for 3D scanning the samples;

Figure 15 is remarkable since it is possible to detect how the flattened sample, in correspondence with the bent line, assumes an "M" shape. The central part of the "M" is a consequence of the bending process, where the tip of the punch induces a concavity upwards. Instead, the two sides of the "M" have a concavity pointing downwards. This is because the first stage of flattening is unbending of the central portion, where the lateral flanges do not remain linear but get bended and curved because of the friction between the sample and lower die and because of their bending stiffness (which is in turn related to the sample slenderness). This phenomenon can be appreciated in Figure 17.

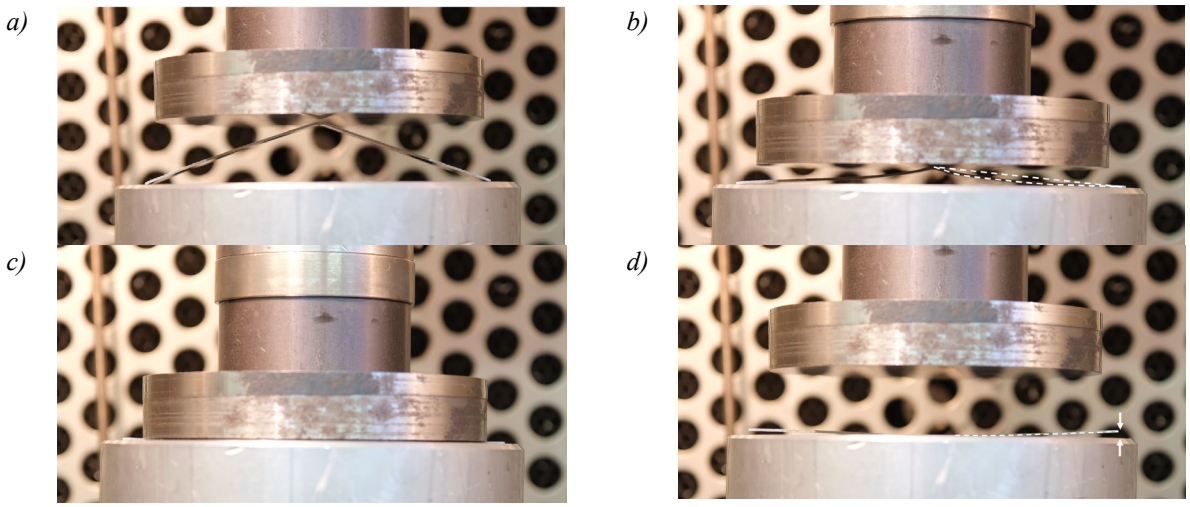

Figure 17. a) Beginning of flattening; b) the un-bending stage of the sample (the lateral flange bends); c) the dwelling stage of flattening (the material gets compressed through the thickness); d) spring-forward effect.

It is noticeable from Figure 17-d that a small spring-forward effect exists. This is because during flattening the sample un-bends and the flanges get a concavity opposite to the one of the central bent line. When the punch continues pushing down the sample, the central bent opens while the lateral flanges are pushed down. But, when the punch force is released, elastic spring-back of the lateral flanges in the proximity of the central bent line takes place. This spring-back is oriented with a concavity pointing upwards, while the spring-back of the central bent line is oriented downwards. The sample globally assumes a "U" shape because of the elastic spring-back of the two regions adjacent to the bent line, while locally, the central part of the specimen assumes an

"M" shape. The spring-forward effect can be quantified quickly through profilometers based on laser sensor technology (Figure 16). The sensor used is a Wenglor MLWI 131 laser profilometer, with a vertical resolution equal to 4.9 µm and the width of the laser is 52 mm. The sensor is actuated by an electric motor and can translate along the Y axis (see Figure 16) while scanning the samples. Different from Alicona, this system is more suited for quick 3D scanning where high resolution or high magnifications are not required. One example of the scanned profile is reported in Figure 18, where a slight non-planarity or spring-forward effect can be appreciated, while in Figure 19 it is possible to appreciate the "M" profile of a remanufactured sample with a double change of concavity and linear trends far from the bent line.

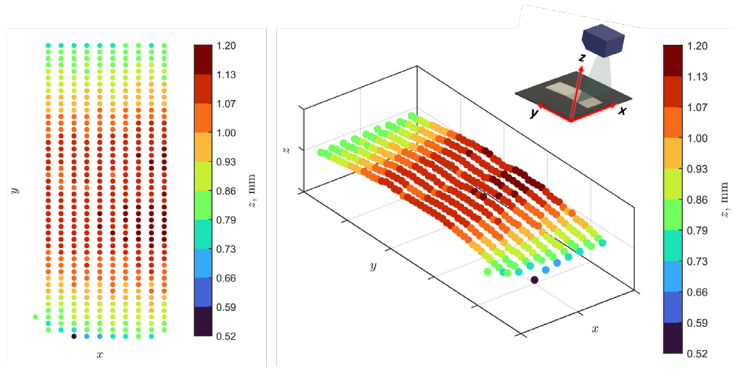

Figure 18. Colour map of the sample is visualized from the top view or isometric view.

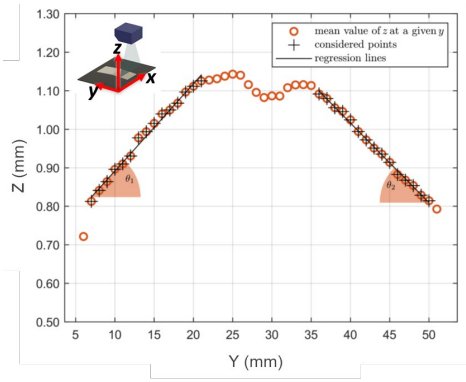

Figure 19. Remanufactured sample scanned with the laser profilometer. This plot is the mean profile of the scan along the X direction.

Figure 17 and Figure 19 might be considered contradictory: in Figure 17-d the flanges are pointing upwards while in Figure 19 downwards. This is because the samples, when measured with the laser profilometer, were placed with the flanges in contact with the support plate, flipping it by 180° after flattening. During the last stage of flattening, when the punch is applying the dwell force, the material gets compressed through the thickness. This can be comprehended by studying the flattening force vs stroke curve of the flattening stage, reported in Figure 20.

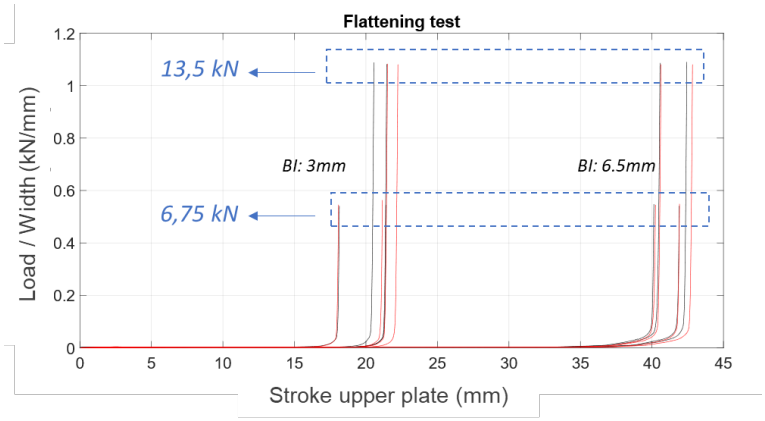

Figure 20. Flattening curve: load/sample width (Y axis) vs stroke of the flattening punch (X-axis).

Figure 20 shows the flattening curves performed in the cold (black lines, 20°C) and warm (red lines, 250°C) processes for two different values of bending index (BI) applied (3 and 6,5 mm). The curves are characterized by two regions: at the beginning the force is almost constant for increasing flattening stroke, corresponding to a limited resisting force exerted by the sample during

the first stage of flattening, i.e. unbending. Secondly, once the sample is completely unbent and flattened, the material gets compressed through the thickness and the plot force vs stroke becomes steep, reminding a sort of coining operation. The decision to test two values of dwell force (one lower and one higher) was intended to comprehend weather the pressing tonnage affects spring-back (or, in this case, spring-forward), since similarly to bending the bottoming phase is needed to calibrate accurately the bent angle. Despite this original thought, it was noticed that using flat dies, to cancel the spring-forward effect a very high tonnage would be required to induce plastic deformation through the thickness. Too high tonnage is unpractical for large samples and would have a double effect. On one hand, it allows having a uniform thickness distribution canceling out the "M" profile. On the other hand, the sample would "spread" laterally because of the high pressure, thus inducing thinning. In this research, the values of forces tested were not enough to induce plastic deformation through the thickness capable of canceling the "M" profile.

Tensile test results.

Following this geometrical explanation of the deformation of the sample, it is clear that the damaged zone of the sample is no longer localized only along the bent line, but also close to it because of the flattening stage. To quantify the effect of the bending and flattening process parameters on the formability of the samples, tensile tests of the remanufactured and reshaped parts were performed. In most cases, the samples failed close to the bent line, indicating that the material underwent damage and strain hardening because of bending, but more importantly, because of the flattening process, where the unbending phase induces such peculiar counter-curvature. This is due to a geometrical effect as explained previously. The tensile engineering stress-strain curves performed are reported in Figure 21. As previously mentioned, from each tensile test, four response variables were extracted: the elongation in correspondence of the max stress (A%), Young's modulus (E), the maximum tensile stress (UTS) and the yielding stress (Ys). To appreciate the effect of the factors tested (BI, DwF, τ, T) on the response variables (A%, E, UTS, and Ys), a scatter plot and a regression model were employed in JMP Software to find possible correlations. For the sake of simplicity, the results of the regression are summarized in Table 1, and relevant scatter plots obtained are reported (namely Figure 23, Figure 24, and Figure 25).

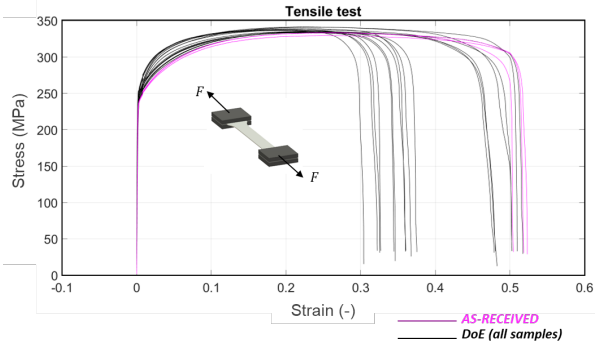

Figure 21. Engineering tensile stress-strain curves for as-received samples (violet) and remanufactured ones (black).

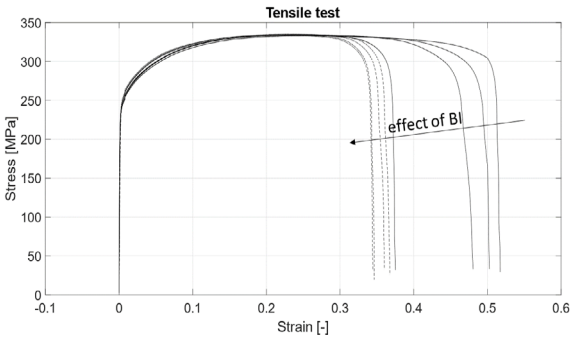

Figure 22. Tensile test of cold-formed and cold-flattened tensile test samples, highlighting the effect of BI.

Filtering Figure 21 by excluding warm-flattened samples and as-received ones, it was possible to obtain Figure 22, where the dashed lines correspond to higher BI values (6.5 mm), i.e. higher punch stroke in the bending stage. The continuous black lines correspond to lower BU values (3 mm). Figure 23 shows how the elongation at maximum stress, which can be at first approximation considered as a formability indicator, decreases for the progressive increase of the bending index. More specifically, the variation in formability can be appreciated in Table 2.

Table 1. Table indicating the presence of correlations between factors (green cells) and response variables (grey cells) indicating the type of trend: increasing (↑), decreasing (↓), multiple (↑↓), or absent (-).

	A%	*E*	*Ys*	*UTS*
BI	↓	-	↑	-
T	↓	↑	↑	↑
τ	-	↑↓	-	-
F	-	-	-	-

Table 2. Variation of elongation at maximum stress according to different forming and reshaping cycles.

Forming and reshaping cycle	A^{*}_{mean} [−]	ΔA^{**}_{mean} (%)
BI 3 mm - cold flattened	0,25	-4,4
BI 3 mm - warm flattened	0,23	-11,8
BI 6,5 mm - cold flattened	0,22	-13,3
BI 6,5 mm - warm flattened	0,19	-25,7
* Mean elongation at maximum stress. ** Variation in percentage of the mean elongation at maximum stress with respect to the "as-received" samples.		

The decrease in A% is caused by the progressive plastic deformation and damage accumulated during forming and flattening. Nevertheless, considering the worst case, for DC04, applying a severe bending and flattening is not decreasing the residual formability in a tremendous amount: the decrement percentage in A% with respect to the "as-received" sample corresponds to values lower (in absolute value) than 26% (Table 2). Therefore, it is reasonable to state that such material, even after severe forming cycles, can be reshaped and reused for a second life where potentially another forming stage can be applied.

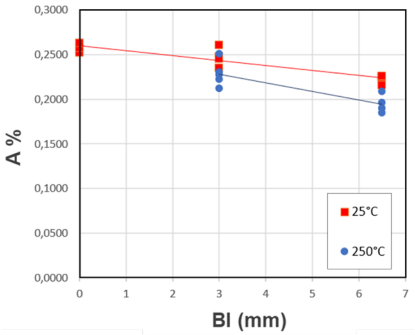

Figure 23. Elongation in correspondence of the max stress (A%) vs bending index (BI) for cold and warm flattened samples.

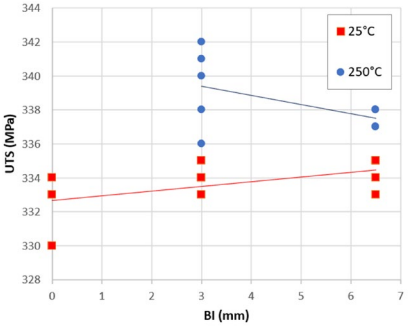

Figure 24. Ultimate tensile stress (UTS) vs bending index (BI) for cold and warm flattened samples.

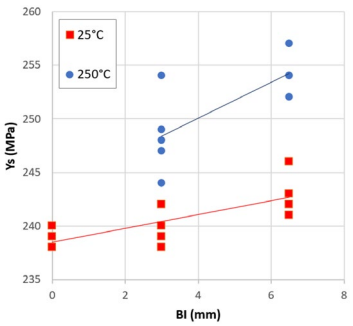

Figure 25. Yielding stress (Ys) vs bending index (BI) for cold and warm flattened samples.

Figure 24 shows how the UTS is approximately constant for increasing bending index, while slightly increasing for warm formed samples. Even though such behavior seems counter-intuitive, it is in line with other studies where temperature can activate thermal aging phenomena, thus modifying the mechanical response of the material [11]. Some mild-steel grades (including DC04) experience also a slight decrease in elongation at fracture when exposed to a range of temperatures between 200 and 400 °C (as observable in Figure 23). Lastly, in Figure 25 it is possible to appreciate the slight increase of yielding stress (Ys) for increasing BI and flattening temperature. The explanation of this behaviour would require some microstructural analysis of the material.

According to Wang et al. in low-carbon steels subjected to warm forming, dynamic strain aging (DSA) phenomena can lead to an increase of micro-hardness and peak stress [17].

Conclusions

The findings presented in this paper contributed to assessing and understanding whether previously bent sheets retain adequate ductility for another forming cycle, a crucial aspect for promoting circular economy practices.

Specifically, the objective of this study is to investigate the plastic deformation and residual formability of DC04 mild steel, a prevalent material used in car bodies. The main idea is to comprehend if stamped steels extracted from end-of-life vehicles could be reshaped or remanufactured providing environmental benefits concerning conventional recycling. Similarly to a former study [11], the flattening process was employed as a reshaping or remanufacturing strategy for recovering the original planar geometry of a V-bent.

To simulate the potential implementation on real car bodies, the experimental procedure involved cold forming samples of 0.8 mm thick DC04 steel into V-bends of varying angles using a controlled punch stroke (Figure 1).

Subsequently, a flattening process was employed to reshape these parts for potential reuse, with key parameters such as dwell force, dwell time, and temperature carefully controlled. Tensile tests (Figure 6) were conducted on both as-received sheets and reshaped samples to understand how work-hardening and residual tensile formability depends on Bending Index (BI), Dwell Force (DwF), Dwell Time (τ), and Flattening Temperature (T). Two levels were tested for each factor (Figure 9), while the response variables of interest were Ultimate Tensile Strength (UTS), Yielding Stress (Ys), Young's Modulus (E), and Elongation at Maximum Stress (A%).

The samples were measured with different techniques before (Figure 10) and after flattening (Figure 14 and Figure 16) in order to comprehend the deformation mechanisms of the material in proximity of the bent line (i.e. the damaged region) and in order to understand the origin of the spring-forward effect (Figure 17). Before flattening Alicona Infinite Focus was employed to measure the external curvature radius and angles of the bent samples. The measurements provided an understandings into the deformation history of the material, providing conclusions in line with the state of the art of sheet metal bending.

Observations during flattening instead are more interesting since this process is novel and employed for remanufacturing already shaped parts. During flattening the bent line unbends and the flange deforms close to the bent line, eventually resulting in a localized permanent deformation and a "M" profile (Figure 15). This mechanism generates in turn a spring-forward effect and globally the samples assumed a "U" shape when the flattening force is released (i.e. when the punch moves upwards, Figure 17).

Analysis of tensile engineering stress-strain curves, scatter plots, and regression models revealed some correlations between the experimental parameters and response variables (Table 1). Particularly, the elongation at maximum stress (A%) decreased with increasing bending index (BI), indicating reduced formability due to accumulated plastic deformation (Figure 23 and Table 2). Ultimate Tensile Strength (UTS) remained relatively constant (Figure 24), while Yielding Stress (Ys) showed a slight increase with a higher Bending Index and flattening temperature (T), as visible in Figure 25. The results are in line with other studies and are explainable by thermal aging, where microstructural modifications induced by the warm flattening stage take place, thus affecting the mechanical properties of the sample.

In conclusion, the results underscored and confirmed the real and concrete possibility of potentially reusing these high-added-value sheets from end-of-life vehicles, presenting a more environmentally sustainable alternative to the prevailing recycling methodologies since they retain adequate residual formability for a second life. This would ensure avoiding the energy-demanding process of metal fusion typical of conventional recycling.

References

[1] J. Pavan Kumar, R. Uday Kumar, B. Ramakrishna, B. Ramu, and K. Baba Saheb, "Formability of sheet metals - A review," *IOP Conf. Ser. Mater. Sci. Eng.*, vol. 455, no. 1, 2018. https://doi.org/10.1088/1757-899X/455/1/012081

[2] N. R. Small, D. K. Williams, R. Roy, and S. K. Hazra, "Accounting for the effect of heterogeneous plastic deformation on the formability of aluminium and steel sheets," *Int. J. Adv. Manuf. Technol.*, vol. 109, no. 1–2, pp. 397–410, 2020. https://doi.org/10.1007/s00170-020-05372-0

[3] S. Dhara, S. Basak, S. K. Panda, S. Hazra, B. Shollock, and R. Dashwood, "Formability analysis of pre-strained AA5754-O sheet metal using Yld96 plasticity theory: Role of amount and direction of uni-axial pre-strain," *J. Manuf. Process.*, vol. 24, pp. 270–282, 2016. https://doi.org/10.1016/j.jmapro.2016.09.014

[4] H. L. Yi, L. Sun, and X. C. Xiong, "Challenges in the formability of the next generation of automotive steel sheets," *Mater. Sci. Technol. (United Kingdom)*, vol. 34, no. 9, pp. 1112–1117, 2018. https://doi.org/10.1080/02670836.2018.1424383

[5] M. Feistle, A. Kindsmüller, I. Pätzold, R. Golle, and W. Volk, "Influence of Sheet Metal Pre-forming on Edge Crack Sensitivity using an AHSS Steel Grade," *Int. J. Mater. Form.*, vol. 15, no. 4, pp. 1–11, 2022. https://doi.org/10.1007/s12289-022-01669-5

[6] D. Lumelskyj, J. Rojek, D. Banabic, and L. Lazarescu, "Detection of Strain Localization in Nakazima Formability Test - Experimental Research and Numerical Simulation," *Procedia Eng.*, vol. 183, pp. 89–94, 2017. https://doi.org/10.1016/j.proeng.2017.04.016

[7] D. Banabic, F. Barlat, O. Cazacu, and T. Kuwabara, "Advances in anisotropy of plastic behaviour and formability of sheet metals," *Int. J. Mater. Form.*, vol. 13, no. 5, pp. 749–787, 2020. https://doi.org/10.1007/s12289-020-01580-x

[8] J. He, Z. C. Xia, X. Zhu, D. Zeng, and S. Li, "Sheet metal forming limits under stretch-bending with anisotropic hardening," *Int. J. Mech. Sci.*, vol. 75, pp. 244–256, 2013. https://doi.org/10.1016/j.ijmecsci.2013.07.007

[9] T. Clausmeyer, M. Noman, and B. Svendsen, "Formulation and application of models for anisotropic hardening in sheet metals subject to complex loading-path changes," *Pamm*, vol. 9, no. 1, pp. 329–330, 2009. https://doi.org/10.1002/pamm.200910138

[10] J. M. Allwood and J. M. Cullen, *Sustainable Materials: With Both Eyes Open*. 2012.

[11] D. Farioli, M. Fabrizio, E. Kaya, M. Strano, and V. Mussi, "Reshaping of thin steel parts by cold and warm flattening," *Int. J. Mater. Form.*, vol. 16, no. 4, 2023. https://doi.org/10.1007/s12289-023-01759-y

[12] D. Farioli, M. Fabrizio, E. Kaya, V. Mussi, and M. Strano, "Energy measurements and LCA of remanufactured automotive steel sheets," in *ESAFORM*, 2023, pp. 1947–1956. doi: 10.21741/9781644902479-210

[13] J. Falsafi, E. Demirci, and V. V. Silberschmidt, "Computational assessment of residual formability in sheet metal forming processes for sustainable recycling," *Int. J. Mech. Sci.*, vol. 119, no. October, pp. 187–196, 2016. https://doi.org/10.1016/j.ijmecsci.2016.10.013

[14] H. Takano, K. Kitazawa, and T. Goto, "Incremental forming of nonuniform sheet metal: Possibility of cold recycling process of sheet metal waste," *Int. J. Mach. Tools Manuf.*, vol. 48, no. 3–4, pp. 477–482, 2008. https://doi.org/10.1016/j.ijmachtools.2007.10.009

[15] Tekkaya, Franzen, and Trompeter, "Wiederverwertungsstrategien für Blechformteile," *SFU*. pp. 187–196, 2008.

[16] R. Bagheriasl, K. Ghavam, and M. J. Worswick, "Formability improvement with independent die and punch temperature control," *Int. J. Mater. Form.*, vol. 7, no. 2, pp. 139–154, 2014. https://doi.org/10.1007/s12289-012-1115-6

[17] Z. Wang *et al.*, "Warm Deformation and Dynamic Strain Aging of a Nb-Cr Microalloyed Low-Carbon Steel," *Metall. Mater. Trans. A Phys. Metall. Mater. Sci.*, vol. 51, no. 9, pp. 4623–4631, 2020. https://doi.org/10.1007/s11661-020-05855-5